RSC Advances

PAPER

View Article Online
View Journal | View Issue

Cite this: *RSC Adv.*, 2025, **15**, 11337

Study on modification and electrochemical properties of COS_2-based cathode materials†

Rongrui Xu,‡ Yicheng Wei,‡ Ling Ding, Hongliang Li, Yuezhen Hua, Yong Cao* and Yanhua Cui *

Thermal batteries are widely used in defense and emergency fields due to their long storage periods and high power characteristics. Among them, cobalt disulfide (CoS_2), as a cathode material, attracts attention because of its high decomposition temperature, excellent discharge capacity, and good electrical conductivity. However, research has found that this material is prone to structural decomposition and phase transition under high-temperature working conditions and long-term storage, leading to critical issues such as electrode activity decay and battery performance degradation. This study innovatively adopts atomic layer deposition (ALD) technology to construct a nanoscale Al_2O_3 coating on the CoS_2 surface, and systematically analyzes it through multi-dimensional characterization methods such as X-ray diffraction (XRD) and scanning electron microscopy (SEM). Experimental results show that after an 8 days simulated storage test, the discharge specific capacity of unmodified CoS_2 decreased to 70% of its initial value, while the Al_2O_3/CoS_2 composite material maintained a capacity retention rate of 90%. This study confirms that Al_2O_3 surface modification technology can effectively inhibit the structural degradation of CoS_2, significantly enhancing the material's environmental tolerance and electrochemical stability.

Received 12th March 2025
Accepted 3rd April 2025

DOI: 10.1039/d5ra01620g

rsc.li/rsc-advances

1. Introduction

Thermal batteries, as non-rechargeable electrochemical devices activated by heat, have become indispensable power sources for military systems such as missiles and torpedoes, as well as critical civilian applications like emergency backup and deep-well drilling, due to their exceptionally long shelf life (5 to 20 years) and instantaneous high-power discharge capability.[1] These batteries operate through thermally activated molten salt electrolytes (*e.g.*, LiCl–KCl, LiBr–LiCl–LiF, *etc.*), maintaining functionality at extreme temperatures, which distinguishes them from traditional energy storage systems.[2]

The cathode material, as the core component of thermal batteries, directly determines the energy density and operational stability of the battery. Transition metal disulfides (FeS_2, CoS_2, *etc.*) have emerged as promising candidates, superior to traditional oxides and halides.[3,4] Notably, CoS_2 exhibits excellent properties, including high theoretical capacity, high decomposition temperature, and metallic-level electronic conductivity.[5,6] However, recent research has shown that CoS_2 undergoes progressive structural degradation both during high-temperature operation and long-term environmental storage. At high temperatures, sulfur loss due to gaseous S_2 emissions leads to phase transitions (*e.g.*, $CoS_2 \rightarrow Co_9S_8$), while room-temperature aging causes surface oxidation and sulfur disproportionation, collectively resulting in capacity fade and voltage fluctuation.[7,8] These issues stem from the inherently weak Co–S bonds and anisotropic lattice expansion during lithiation/delithiation.[9] Despite its technical urgency, the atomic decomposition pathways of CoS_2 remain poorly understood, with limited strategies to mitigate its instability.[10,11]

Existing methods, such as particle size optimization or elemental doping (*e.g.*, with Ni, Cu), can only partially inhibit sulfur sublimation but fail to address interfacial corrosion mechanisms.[12,13] Moreover, most stability assessments neglect

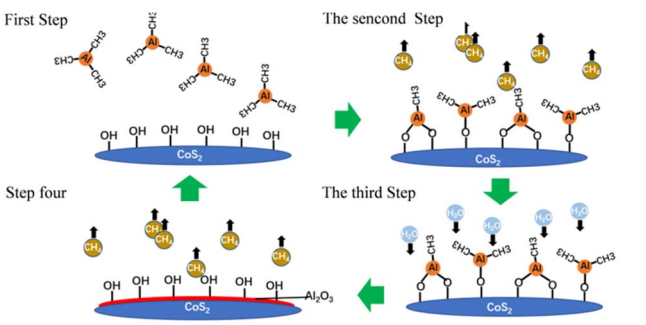

Fig. 1 Schematic of the ALD preparation CoS_2@Al_2O_3 process.

Institute of Electronic Engineering, China Academy of Engineering Physics, Mianyang 621900, P. R. China. E-mail: cuiyanhua@netease.com

† Electronic supplementary information (ESI) available. See DOI: https://doi.org/10.1039/d5ra01620g

‡ These authors contributed equally to this work.

the coupling effects between thermal cycling and environmental aging, leading to an overestimation of performance in practical scenarios.[14,15] In our previous study, it was demonstrated that CoS_2 modified with Al_2O_3 nanoparticles synthesized *via* a facile wet-chemical method exhibits exceptional electrochemical performance. To further investigate whether analogous enhancement effects can be achieved through the deposition of Al_2O_3 thin films *via* atomic layer deposition (ALD) or magnetron sputtering, this work systematically explores the interfacial engineering and electrochemical mechanisms of these vapor-phase fabricated Al_2O_3/CoS_2 heterostructures.[16] To address these gaps, we propose an innovative approach: coating CoS_2 particles with an Al_2O_3 layer using atomic layer deposition (ALD) technology. The Al_2O_3 coating is hypothesized to serve as a physical barrier that mitigates adverse interfacial reactions and structural collapse during thermal cycling and long-term storage. Systematic studies, including X-ray diffraction (XRD), thermogravimetry (TG), and scanning electron microscopy (SEM), were conducted to elucidate the structure and thermal stability of the modified material. Surprisingly, after 8 days of simulated storage testing, alumina-coated cobalt disulfide retained 90% of its initial discharge capacity, while the uncoated cobalt disulfide significantly dropped to 70%. These findings emphasize the effectiveness of alumina coating in maintaining the electrochemical integrity of cobalt disulfide, providing a material-level solution for enhancing the longevity and reliability of the next generation of thermal batteries. This work opens the path for designing robust electrode materials suitable for energy storage systems in extreme conditions.

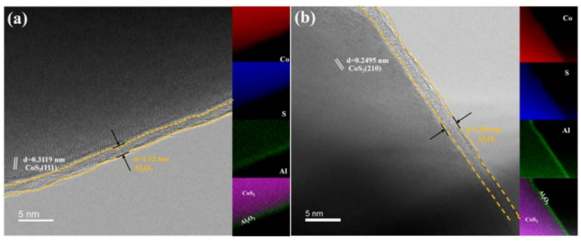

Fig. 3 TEM images: (a) Al_2O_3@CoS_2-10s; (b) Al_2O_3@CoS_2-30s.

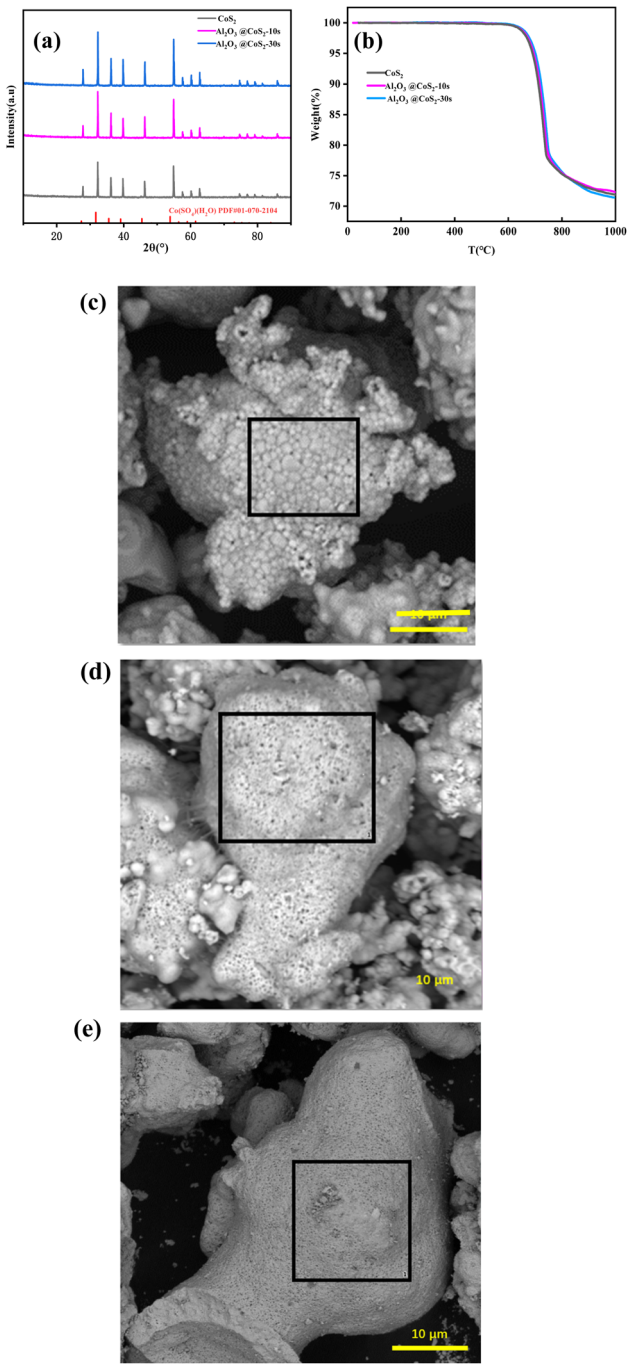

Fig. 2 CoS_2, Al_2O_3@CoS_2-10s, Al_2O_3@CoS_2-30s: (a) XRD Patterns; (b) TG Curves; (c–e) EDS elemental distribution maps of Al_2O_3@CoS_2-10s, Al_2O_3@CoS_2-30s, and CoS_2.

2. Experimental

2.1 Material preparation

TIn this study, CoS_2 material was purchased from Central South University with a purity of 99.9%. An Al_2O_3 coating was prepared on the surface of the CoS_2 electrode through atomic layer deposition (ALD). The deposition temperature ranged from 250–300 °C. Trimethylaluminum ($Al(CH_3)_3$) was used as the precursor for depositing Al_2O_3, with a pulse time of 0.06 seconds and an N_2 purge time of 30 seconds. After completing

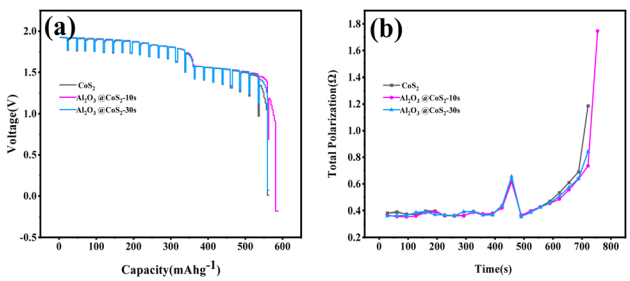

Fig. 4 Comparison of discharge performance among CoS_2, Al_2O_3@CoS_2-10s, and Al_2O_3@CoS_2-30s: (a) specific capacity diagram; (b) polarization internal resistance diagram.

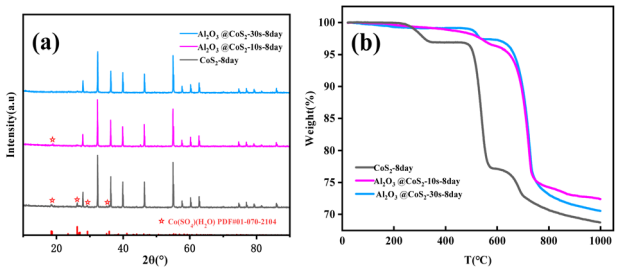

Fig. 5 CoS_2, Al_2O_3@CoS_2-10s, Al_2O_3@CoS_2-30s: (a) TG curves; (b) XRD patterns.

10 cycles and 30 cycles, two types of CoS_2 materials with different coating amounts were obtained, denoted as Al_2O_3@CoS_2-10s and Al_2O_3@CoS_2-30s, respectively.

2.2 Material characterization

The X-ray diffractometer (XRD) was used to collect the XRD pattern information of the tested samples at room temperature (scan range: 10–90°, heating rate: 10 K min^{-1}, scan speed:16° min^{-1}; atmosphere:Ar). Scanning Electron Microscopy (SEM) was employed to observe the morphology of the CoS_2 material. Elemental distribution characterization of the samples was performed using an Energy Dispersive X-ray Spectrometer (EDS). A synchronous thermal analyzer was used to collect the TG-DSC information during the thermal decomposition process of CoS_2 (heating rates: 5, 10, 15, 20 K min^{-1}; atmosphere: N_2; gas flow rate: 120 ml min^{-1}; temperature range: 30 °C to 1000 °C).

2.3 The single thermal battery fabrication and measurements

All pretreatment operations for electrode materials were conducted inside a glove box filled with Ar atmosphere. The anode (0.52 g) was LiB alloy (55 wt% Li, Ruilin), the separator (0.8 g) consisted of 50 wt% electrolyte (45 wt% LiCl-55 wt% KCl) and 50 wt% MgO and the cathodes (0.4 g) consisted of 80 wt% active material and 20 wt% electrolyte, all were stacked to form a cell of 32 mm under a pressure of 120 MPa in a drying room with a dew-point temperature below −50 °C. The single cells were discharged at 500 °C with a constant current of 100 mA cm^{-2} (with a period of 30 s) and a pulsed current of 500 mA cm^{-2} (with a period of 1 s) using a Land battery test system (CT2001A, LAND). The total polarization, that is the resistance of a single thermal battery (Rb), is calculated as follows.

3. Results and discussion

Fig. 2a presents the X-ray Diffraction (XRD) patterns of CoS_2, Al_2O_3@CoS_2-10s, and Al_2O_3@CoS_2-30s. All three samples exhibit characteristic peaks of CoS_2 without the appearance of any impurity phases, indicating that the coated materials have not undergone decomposition. However, the characteristic peaks of Al_2O_3 are not observable in the Al_2O_3@CoS_2 samples, which is attributed to the very thin layer of Al_2O_3 deposited by ALD or the amorphous nature of the coated Al_2O_3. Fig. 1b displays the Thermogravimetric (TG) curves of the three samples, with thermal decomposition temperatures all at 650 °C. The coating of Al_2O_3 does not alter the thermal decomposition temperature of the material, making it suitable as a cathode material for thermal batteries. SEM (Scanning Electron Microscope) and EDS (Energy Dispersive Spectrometer) analyses were conducted to investigate the morphology and surface element composition of CoS_2, Al_2O_3@CoS_2-10s, and Al_2O_3@CoS_2-30s, as shown in Fig. 2. Compared to the raw material, the morphologies of Al_2O_3@CoS_2-10s and Al_2O_3@CoS_2-30s coated by ALD do not change, further confirming that the thickness of the coating layer is at the nanoscale and thus not discernible in SEM images. However, EDS clearly shows the

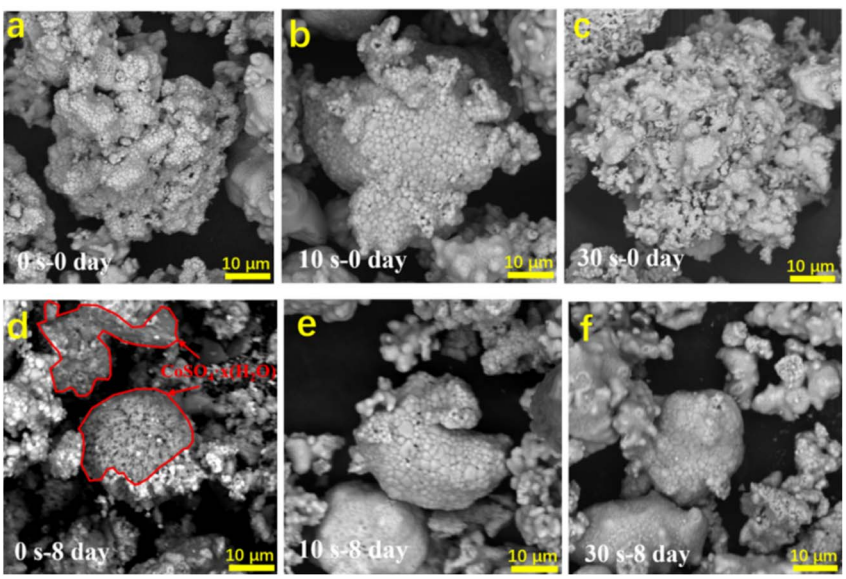

Fig. 6 Comparison of CoS_2 before and after storage: (a and d); Comparison of Al_2O_3@CoS_2-10s before and after storage: (b and e); Comparison of Al_2O_3@CoS_2-30s before and after storage: (c and f).

uniform distribution of Al and O on the particle surface with a consistent distribution pattern, indicating the presence of an Al_2O_3 coating layer on the surface of CoS_2.

To further investigate whether Al_2O_3 was successfully synthesized and coated on the surface of CoS_2, we characterized the coated samples using TEM, with the results presented in Fig. 3. Through EDS scanning analysis, the upper left section of Fig. 3a and the lower left section of Fig. 3b depict CoS_2 particles. Calculations reveal that the interplanar spacings are 0.3119 nm and 0.2495 nm, corresponding to the (111) and (210) crystal planes of CoS_2, respectively. A uniform layer of amorphous Al_2O_3 is coated on the surface of CoS_2. The thickness of the Al_2O_3 coating after 10 cycles is 1.12 nm, and after 30 cycles, it is 1.89 nm, indicating that a greater number of cycles results in a thicker Al_2O_3 coating.

Three materials, namely CoS_2, Al_2O_3@CoS_2-10s, and Al_2O_3@CoS_2-30s, were used to fabricate thermal battery cells for pulse discharge testing at 500 °C. The discharge conditions were as follows: a background current of 100 mA cm^{-2} was applied for 30 seconds, followed by a pulse current of 500 mA cm^{-2} for 1 second. Fig. 4 shows that the first discharge voltage platform for all three materials is approximately 1.9 V, with a discharge capacity of around 500 mA h g^{-1} when the voltage drops to 1.5 V. The polarization internal resistance is also nearly identical. This indicates that coating with Al_2O_3 has no significant effect on the discharge voltage or electrical conductivity of CoS_2.

After storing the three materials, namely CoS_2, Al_2O_3@CoS_2-10s, and Al_2O_3@CoS_2-30s, in air at a constant temperature of 25 °C with 70% relative humidity for 8 days, they were then vacuum-dried at 100 °C for 24 hours. These samples are

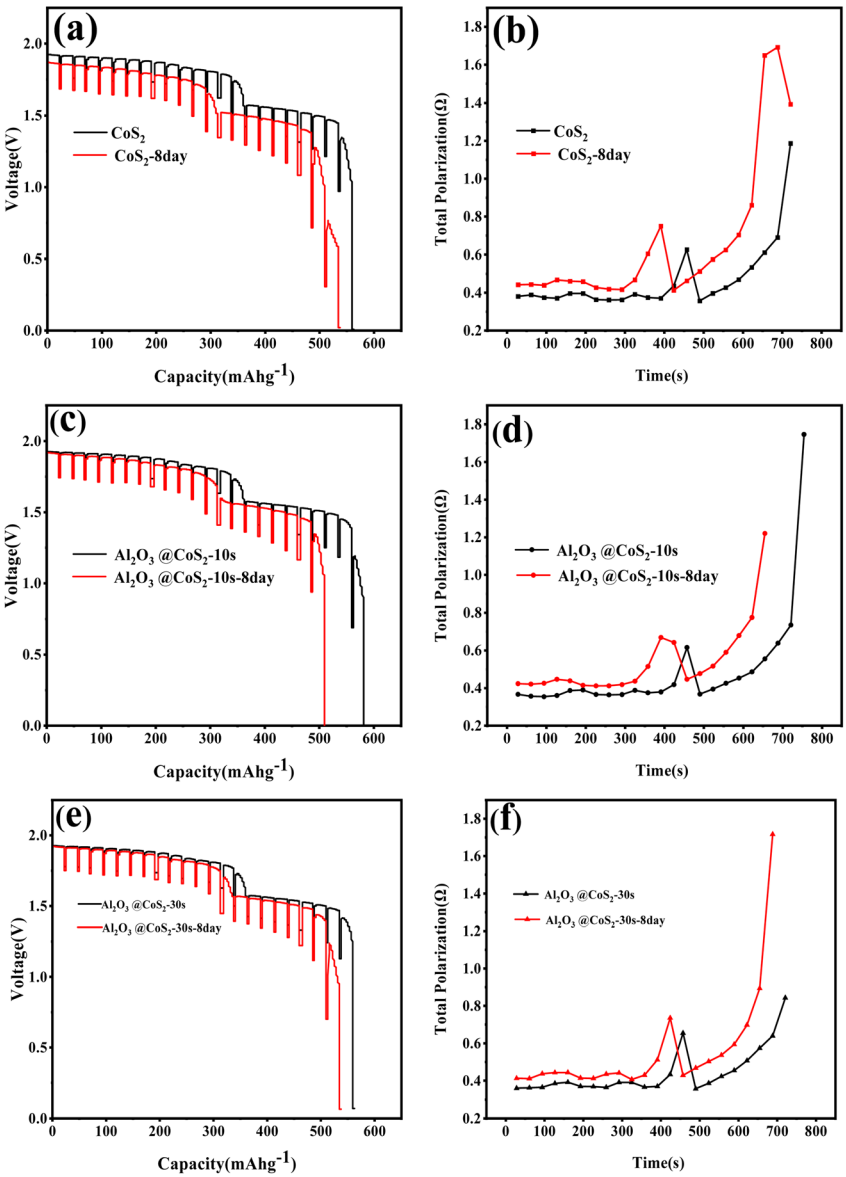

Fig. 7 (a) Fig. 6 displays the specific capacity and polarization internal resistance graphs for CoS_2-8day (a and b), Al_2O_3@CoS_2-10s-8day (c and d), and Al_2O_3@CoS_2-30s-8day (e and f) respectively.

hereafter referred to as CoS_2-8day, Al_2O_3@CoS_2-10s-8day, and Al_2O_3@CoS_2-30s-8day, respectively. Fig. 5a presents the XRD patterns of the stored samples. The uncoated raw material exhibits obvious characteristic peaks of $CoSO_4 \cdot H_2O$ after storage, indicating decomposition of the material. Although Al_2O_3@CoS_2-10s-8day also shows characteristic peaks of $CoSO_4 \cdot H_2O$, the intensity of these peaks is very weak. In contrast, Al_2O_3@CoS_2 does not exhibit any characteristic peaks of $CoSO_4 \cdot H_2O$, suggesting no decomposition or minimal decomposition. Both observations demonstrate that coating CoS_2 with Al_2O_3 using ALD technology can significantly enhance the storage stability of CoS_2.

Fig. 5b displays the TG curves of the three materials after storage. All three materials undergo decomposition after 8 days of storage; however, compared to the raw material, the degree of decomposition of the Al_2O_3@CoS_2 coated samples is greatly reduced, with Al_2O_3@CoS_2-30s exhibiting the lowest degree of decomposition. The mass percentages corresponding to the thermal decomposition platform of CoS_2 are 78 wt%, 95 wt%, and 97 wt%, respectively. The comparison of storage stability under the same conditions is as follows: CoS_2 < Al_2O_3@CoS_2-10s < Al_2O_3@CoS_2-30s.The atomic layer deposition (ALD)-engineered nanoscale Al_2O_3 coating on the CoS_2 surface consists of an ultrathin protective layer, which accounts for the nearly identical final residual mass percentages observed in thermogravimetric (TG) analysis. In contrast, the uncoated pristine CoS_2 exhibited an earlier decomposition temperature due to the absence of this protective barrier, rendering it more susceptible to thermal degradation. This observation further demonstrates that the Al_2O_3-coated CoS_2 significantly enhances the stability of thermal batteries, as evidenced by the delayed decomposition behavior and improved electrochemical performance.

Fig. 6 presents comparative SEM images of CoS_2-8day, Al_2O_3@CoS_2-10s, and Al_2O_3@CoS_2-30s before and after 8 days of storage. After storage, decomposition products ($CoSO_4 \cdot H_2O$, highlighted in red regions) were observed on the surface of uncoated CoS_2 particles. In contrast, comparative analysis of images e and f reveals no significant degradation for the Al_2O_3-coated samples under identical storage conditions, further confirming that the ALD-deposited Al_2O_3 layer significantly enhances the storage stability of CoS_2. Supporting high-magnification SEM images (provided in the ESI†) unambiguously verify the presence of $CoSO_4$ on the CoS_2 surface, corroborating the role of the Al_2O_3 coating in mitigating degradation.

As shown in Fig. 7, a comparison of the discharge performance of the three materials after 8 days of storage reveals the following: the first platform voltage of CoS_2-8day, Al_2O_3@CoS_2-10s-8day, and Al_2O_3@CoS_2-30s-8day decreased by approximately 0.1 V, 0.03 V, and 0.01 V, respectively, compared to before storage. The discharge specific capacities at 1.5 V decreased by about 30%, 16%, and 10%, respectively. The polarization internal resistances increased by approximately 0.07 Ω, 0.05 Ω, and 0.05 Ω, respectively. These results indicate that coating with Al_2O_3 significantly enhances the storage stability of CoS_2.

The reasons why coating CoS_2 with Al_2O_3 using ALD improves its storage stability without compromising its discharge performance and thermal stability may be as follows: the ALD coating method results in a uniform and very thin (nanoscale) protective layer of Al_2O_3 on the surface of CoS_2. This layer effectively reduces the contact between H_2O and CoS_2, thereby lowering the rate of decomposition of CoS_2 when exposed to water and oxygen, and ultimately enhancing storage stability. At high temperatures, due to thermal expansion and contraction or the insertion of lithium ions into Al_2O_3@CoS_2, the particles of the Al_2O_3@CoS_2 cathode material expand, causing the surface Al_2O_3 layer to crack. This allows lithium ions to normally insert into CoS_2 during discharge, thus not affecting the discharge performance of CoS_2. Additionally, since the thermal decomposition temperature of Al_2O_3 is much higher than that of CoS_2, the thermal stability of the Al_2O_3@-CoS_2 composite material remains unchanged.

4. Conclusions

Addressing the issue of insufficient stability in CoS_2 materials, this study employed Atomic Layer Deposition (ALD) to uniformly coat a thin layer of Al_2O_3 on the surface of CoS_2, successfully fabricating a protective layer that is both uniform and of minimal thickness. Experiments revealed that this composite material maintains a high degree of consistency with the original CoS_2 material in terms of micromorphology, thermogravimetric analysis, and discharge performance, indicating that the Al_2O_3 layer does not compromise its excellent properties. Furthermore, storage tests found that the unprotected CoS_2 material exhibited a significant decrease of 30% in discharge specific capacity and an increase of 0.07 Ω in polarization internal resistance after being stored for 8 days, demonstrating notable performance degradation. In contrast, the CoS_2 composite material coated with 30 layers of Al_2O_3 on its surface showed only a 10% decrease in discharge specific capacity and a smaller increase in polarization internal resistance of just 0.05 Ω under the same storage conditions. This suggests that the Al_2O_3 protective layer effectively isolates CoS_2 from direct contact with moisture in the air, thereby substantially enhancing the material's storage stability. Therefore, the Al_2O_3@CoS_2 composite material outperforms bare CoS_2 in terms of storage stability.

Data availability

The data supporting this article have been included as part of the manuscript.

Author contributions

Rongrui Xu and Yicheng Wei: data curation, formal analysis, investigation, writing-original draft, writing-review & editing; Ling Ding: writing-original draft; Hongliang Li: formal analysis; Huazhen Hua: supervision; Yong Cao: supervision, project administration; Yanhua Cui: Supervision, project administration, funding acquisition.

Conflicts of interest

There are no conflicts to declare.

Acknowledgements

This work is financially supported by the National Natural Science Foundation of China (Grant No. 52474335).

Notes and references

1 R. A. Guidotti and P. Masset, Thermally activated ("thermal") battery technology: Part I: An overview, *J. Power Sources*, 2006, **161**(2), 1443–1449.
2 R. A. Guidotti, *Thermally-related Safety Issues Associated with Thermal batteries*, SAND2006-1902, Sandia National Laboratories (SNL), Albuquerque, NM, and Livermore, CA (United States), 2006.
3 W. Su, M. Chen, Z. Wang, *et al.*, Failure Mechanism and Residual Stress Analysis of Crystal Materials for the Thermal Battery, *Crystals*, 2024, **14**(2), 20.
4 P. Masset and R. A. Guidotti, Thermal activated (thermal) battery technology: Part II. Molten salt electrolytes, *J. Power Sources*, 2007, **164**(1), 397–414.
5 R. A. Guidotti and P. Masset, Thermally activated ("thermal") battery technology: Part I: An overview, *J. Power Sources*, 2006, **161**(2), 1443–1449.
6 K. Bateman, R. K. B. Gover and J. T. S. Irvine, *Novel Thermal Batteries Based on Sodium Chemistries*, ECS Meeting Abstracts, 2023.
7 Jr W. Rogers, S. J. Ward and R. A. Guidotti, *Sandia Report SAND84-0236*, April, 1984.
8 R. A. Guidotti and F. W. Reinhardt, *Sandia Report SAND83-2270*, July, 1985.
9 R. A. Guidotti, F. W. Reinhardt and D. R. Tallant, *Sandia Report SAND83-2272*, June, 1984.
10 P. J. Masset and R. A. Guidotti, Thermal activated ("thermal") battery technology: Part IIIa: FeS2 cathode material, *J. Power Sources*, 2008, **177**(2), 595–609.
11 O. Kubaschewski, C. B. Alcock and P. J. Spencer, *Materials Thermochemistry*, Pergamon Press Ltd, Headington Hill Hall, Oxford OX 3 0 BW, UK, 1993, p. 363.
12 S. S. Wang and R. N. Seefurth, Electrochemical Studies of FeS2 Electrodes in Various Sulfide-Containing Molten Salts, *J. Electrochem. Soc.*, 1987, **134**(3), 530.
13 Z. Tomczuk and D. R. Vissers, EMF Measurements on Select Transitions of the Li-Al/FeS2 System, *J. Electrochem. Soc.*, 1986, **133**(12), 2505.
14 R. A. Guidotti, F. W. Reinhardt and J. Odinek, Overview of high-temperature batteries for geothermal and oil/gas borehole power sources, *J. Power Sources*, 2004, **136**(2), 257–262.
15 P. J. Masset and R. A. Guidotti, Thermal activated ("thermal") battery technology: Part IIIa: FeS2 cathode material, *J. Power Sources*, 2008, **177**(2), 595–609.
16 P. Yang, X. C. Zhang, C. G. Zhang, S. P. Ma, X. W. Yang, Y. L. Xiong, Y. Xie, Y. Cao, Y. H. Cui, X. J. Liu and X. L. Li, *J. Power Sources*, 2021, **511**(8), 230424.